High Heat-Flux Sensor Calibration: A Monte Carlo Modeling

A. V. Murthy*
Aero-Tech, Inc., Hampton, Virginia 23666-5528
and
A. V. Prokhorov† and D. P. DeWitt‡
National Institute of Standards and Technology, Gaithersburg, Maryland 20899-8441

**Conventional calibration of heat-flux sensors uses high-temperature blackbody radiation and places the sensors away from the blackbody aperture. This approach limits the achievable calibration heat flux to about 50 kW/m².
Recent interest in extension of the calibration to higher heat-flux levels requires placement the sensors inside the heated cavity under nearly hemispherical irradiation environment. The incident flux at the sensor location depends on the effective emissivity, which is a function of the combined cavity and sensor geometry, and the properties of the radiating surfaces. A scheme is presented to compute the effective emissivity for such measurement schemes by the use of the Monte Carlo technique. Typical results presented demonstrate the influence of the cavity wall surface emissivity and diffusity, nonuniform temperature distributions, and the sensor location on the calculated effective emissivity. The computations show that the optimum location for the sensor is at a distance of about one cavity radius from the cavity bottom. The effective emissivity at this location has a high value, even in the presence of a linear wall-temperature variation, and is relatively insensitive to the cavity-wall temperature gradient. The use of a reflecting shield to increase the effective emissivity is also investigated.**

Nomenclature

B = hemispherical radiative flux
D = diffusity
d = diameter
L = cylindrical cavity length
T = temperature, K
x = distance from cavity base to sensor
Δ = incremental change
ε = emissivity
ρ = reflectance
σ = Stefan–Boltzmann constant

Subscripts

a = ambient conditions
b = refers to cavity bottom
c = refers to cavity
e = refers to cavity exit
eff = effective value
h = sensor-holder surface
iso = isothermal conditions
ref = reference value
s = refers to sensor
sh = refers to reflecting shield

Introduction

THE use of blackbody radiant sources is ubiquitous in radiation thermometry. Practical blackbody sources have an effective emissivity of nearly unity over a wide spectral range when observed normally or within a narrow view angle as in radiometric applications. Typical applications are in radiance temperature measure-

ments and photometry, where the measuring instrument is located far away from the blackbody aperture. The effective emissivity will be nearly unity for the viewing conditions, but the associated irradiance will be small. Another important application of the blackbody radiation is in the calibration of heat-flux sensors.[1,2] These sensors, typically used in aerospace applications and fire research, operate at irradiance or heat-flux levels from about $50 \text{ kW} \cdot \text{m}^{-2}$ to in excess of $1000 \text{ kW} \cdot \text{m}^{-2}$, much higher than encountered in radiance temperature calibrations. Blackbody sources can deliver such high heat-flux levels with the upper limit given by the Stefan–Boltzmann equation corresponding to the cavity temperature. However, calibration at high heat-flux levels requires placement of the sensors close to the blackbody aperture or even inside the cavity.

This situation leads to large view angles, hemispherical when inside the cavity between the sensor and the radiating source. Moreover, the proximity of a sensor to the heated cavity walls results in radiation heat exchange between the walls and the cold sensor-holder assembly. Factors such as the absorptance of the sensor coating, the cavity-wall emissivity, and the non-uniform temperature distribution of the source tend to reduce the effective emissivity at the measurement location from the theoretical value of unity. The determination of the effective emissivity and the incident radiation at the sensor location requires that account be taken for all of the aforementioned factors.

Accurate experimental determination of the effective emissivity of the radiating cavities is difficult. Therefore, considerable attention is devoted to the calculation of effective emissivity by analytical or numerical methods. The calculations for the isothermal and nonisothermal cavities with diffusely emitting and reflecting walls are amenable to analysis by the use of various methods for numerical solution of radiation heat transfer integral equations.[3] In the last two decades, the Monte Carlo method has emerged as a powerful tool for effective emissivities computation of cavities having complicated shapes and diffuse or specular-diffuse walls.[4−9] However, most of these studies are applicable to conditions when the view is from outside of the blackbody aperture.

This paper presents an application of the Monte Carlo method and appropriate software[10] to calculate the effective emissivity for locations inside cylindrical cavity. Most of the high-temperature blackbodies in use are of cylindrical shape and made of graphite material. The test configuration corresponds to a sensor-holder assembly placed at different locations inside the heated cavity. The analysis models the cavity-sensor assembly as a closed, nonisothermal

*President and Contractor.
†Contractor, Optical Technology Division.
‡Faculty Staff, Optical Technology Division.

enclosure with an infinitesimally small aperture at the sensor location. The following sections give a brief description of the method, along with typical results showing the effect of the sensor holder to cavity diameter ratio, walls emissivity and diffusity, and nonuniform temperature distribution along the cavity internal surface.

Method of Computations

The STEEP3 program uses the Monte Carlo method[9–11] to calculate the spectral and total effective emissivity of axisymmetric cavity shapes, formed by rotation of a nonself crossing polygonal line around the axis of symmetry. The method assumes uniform optical properties across each surface that corresponds to the ith segment of the generatrix. Each surface emits diffusely (according to Lambert's law), with an emissivity ε_i. According to the specular-diffuse reflection model employed, the directional–hemispherical reflectivity $\rho_i (= 1 - \varepsilon_i)$ is independent of the angle of the radiation incidence, and the reflected radiation is the sum of diffuse and specular components for each angle of incidence. The value of diffusity D_i (not to be confused with diffusivity) of the ith surface, representing the ratio of diffusely reflected energy to the full energy reflected over the hemispherical solid angle, is also independent of the incidence angle.

The analysis based on ray optics does not consider the diffraction losses at the aperture edges and assumes that the polarization effects are negligible due to multiple reflections in the cavity. The effective emissivity of a cavity depends on the viewing solid angle at the observation point. For the present problem, the view angle is hemispherical. Therefore, for a nonisothermal cavity, the corresponding hemispherical effective emissivity is

$$\varepsilon_{\mathrm{eff}}(T_{\mathrm{ref}}) = B \big/ \sigma T_{\mathrm{ref}}^4$$

For a nonisothermal cavity, the value of B is the superposition of thermal radiation fluxes from surfaces having different temperatures and fluxes transferred by multiple reflections; thus, the unambiguous determination of T_{ref} is impossible. The computed value of $\varepsilon_{\mathrm{eff}}$ depends on the choice of T_{ref}, which is arbitrary and is a conditional quantity important only for the fulfillment of the relationship

$$\varepsilon_{\mathrm{eff}}(T_{\mathrm{ref},1}) T_{\mathrm{ref},1}^4 = \varepsilon_{\mathrm{eff}}(T_{\mathrm{ref},2}) T_{\mathrm{ref},2}^4$$

The program uses the principle of optical reciprocity and a backward ray tracing technique to calculate the effective emissivity. A recent work[12] demonstrates the equivalence of the backward ray tracing technique with the forward ray tracing, where ray trajectories originate at the emitting surface of the cavity.

Consider the sensor-holder assembly inserted into the radiating cavity. It is possible to obtain a new cavity configuration by replacement of the annular gap between the cavity aperture and the sensor's holder by a virtual black surface at environmental temperature T_a and to make a centrally positioned circular opening of small radius on the sensor surface. The new configuration consists of both real and virtual surfaces and has a tiny aperture in the center of the sensor. With the new cavity configuration, it is possible to compute the hemispherical effective emissivity by the use of the STEEP3 program. We required that the small virtual opening does not disturb the radiation field inside the cavity. This hypothesis supposes that the effective emissivity for hemispherical irradiation at the sensor's center must be the same as the hemispherical effective emissivity of the small opening in the sensor's center. The calculations are valid when the distance between the sensor location and the cavity end is larger than the virtual aperture radius.

Computational Model

Figure 1 shows a typical calibration arrangement and the corresponding modeling geometry used in the computations. The blackbody-aperture diameter is the same as the cavity diameter for the present analysis. The water-cooled sensor mounted at the tip of a long holder is placed inside the heated cavity during calibration (Fig. 1a). With the observation point inside the cavity, the field of view is hemispherical for the arrangement shown. This arrangement
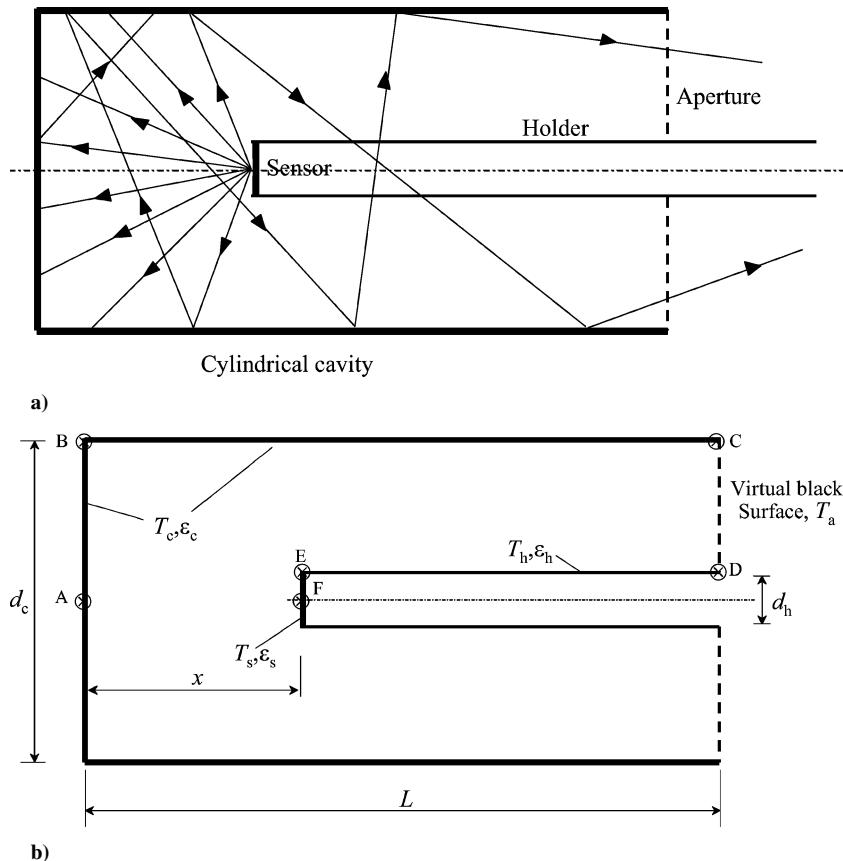

Fig. 1   Modeling for Monte Carlo calculations: a) typical experimental arrangement and b) closed enclosure model.

Table 1 Initial data for numerical modeling

Parameter	Value(s)
Cylindrical cavity length L	5
Cylindrical cavity diameter d_c	1
Sensor-holder diameter d_h	0.25, 0.50, 0.75
Sensing region diameter d_s	0.125, 0.25, 0.5
Distance from sensor to cavity bottom	0 to 5
Emissivity of graphite cavity walls ε_c	0.7, 0.8, 0.9
Diffusity of graphite cavity walls D_c	0.5, 0.75, 1
Emissivity of sensor holder ε_h	0.5
Diffusity of sensor holder D_h	0
Emissivity of sensor receiving area ε_s	0.95
Diffusity of sensor receiving area D_s	1
Reference temperature T_{ref}, K	1000
Cavity bottom temperature T_b, K	1000
Cavity edge temperature T_e, K	1000, 980, 960, 940
Sensor-holder temperature T_h, K	300
Sensor temperature T_s, K	300
Ambient temperature T_a, K	300

is in contrast to conventional usage of blackbodies with the observation point located outside the blackbody aperture. Most of the software programs, including STEEP3, analyze conventional configurations only. Figure 1b shows the cavity-sensor-holder modeling used to adapt the STEEP3 program for the present analysis with the observation point inside the cavity.

The computational model (Fig. 1b) represents the boundary consisting of the blackbody cavity (A–C), sensor-holder (D–E), and the annular opening at the blackbody exit (C–D) as a closed enclosure, with a vanishingly small aperture at the sensor (F). The temperature distribution and the emissivity along the various segments of the closed boundary can be either uniform or varying to represent both isothermal and nonisothermal conditions of the radiating cavity. A virtual black surface at ambient temperature representing the annular area at the cavity exit completely absorbs the radiation escaping from the cavity.

Table 1 lists the values of the various parameters used in the numerical modeling. All geometrical parameters represent the relative units of length. The cylindrical cavity geometry had a length-to-diameter (L/d_c) ratio of five, which is representative of the high-temperature graphite blackbody geometry currently in use for experimental evaluation studies. The sensor-holder diameter (d_h) values in the modeling corresponded to holder-to-cavity diameter ratios (d_h/d_c) of 0.25, 0.50, and 0.75. The location of the sensor is at the center of the holder end surface. The sensing area is usually small, but the entire end surface is usually painted with high absorptance paint. However, the present calculations consider cases with the full, as well as a smaller region covered with high absorptance paint. The sensor location inside the cavity varied from the cavity bottom to the exit.

The emissivity of the graphite material, used in the manufacture of high-temperature blackbodies, varies widely depending on the grade of the material. Hence, three nominal values of cavity surface emissivity $\varepsilon_c = 0.7$, 0.8, and 0.9 were chosen for the calculations. The angular distribution of radiation reflected from graphite surface depends on its roughness, wavelength, and other factors. Significant peaks of specular reflection are observable only for grazing incidence angles and in the far-infrared region. We assumed that the cavity walls reflect diffusely ($D = 1$). The influence of the specular component was evaluated separately.

The temperature distribution along the cavity base (A–B) and length (B–C) was either uniform for the isothermal-cavity conditions, or linearly varying to represent the temperature gradient effects. The temperature of the virtual black surface (C–D) was set equal to the ambient value of 300 K.

After insertion of the sensor-holder assembly inside the heated cavity, the rise in sensor temperature is not significant due to water cooling. The holder will normally have a polished surface, and the sensor surface coated with high absorptance paint. Therefore, the temperature of the sensor and the holder were also considered to be

at ambient value, along with typical emissivity values of $\varepsilon_h = 0.5$ and $\varepsilon_s = 0.95$, respectively.

The cooled sensor-holder assembly, when inserted into the cavity, causes an increase in the blackbody heating power that is necessary to reach a given mean cavity temperature. However, the blackbody control system regulates the cavity temperature by maintaining the cavity-bottom temperature at the set value. The temperature distribution along the cavity depends on details of the design of the graphite heating element, the outer insulation, and the blackbody cooling arrangement. The related heat transfer process can be quite complex and needs experimental evaluation for the particular blackbody facility to determine the furnace loading. A simplistic approach is to assume that the heat losses are nearly same along the cavity length when the sensor is close to the cavity bottom, with the consequent effect on the shape of temperature distribution small. Therefore, we modeled the cavity-wall temperature gradient effect by considering the isothermal bottom at T_b, where the temperature is controlled, and a linear drop along cylindrical generatrix down to temperature T_e at the cavity edge.

Numerical Results and Discussion

The accuracy of effective emissivity calculations by the use of the STEEP3 program depends on two parameters: uncertainty due to truncation of ray trajectories, which determines the minimal radiation flux transferred by ray tracing, and the random error that decreases with an increase in the number of rays traced. From a series numerical experiments, we found that employing 10^7 rays ensures a random component of uncertainty less than 10^{-4} from the computed value of the effective emissivity for $\varepsilon_{\text{eff}} > 0.95$. We set the uncertainty due to truncation of ray trajectories at 10^{-5} from the initial radiance of a ray.

Preliminary numerical experiments showed that, for values of the virtual aperture to blackbody cavity-diameter ratio less than 0.001, the equivalent cavity behaves like an absolute closed cavity with no significant change in the computed effective emissivity.

Isothermal Cavity

First, the isothermal case with the cavity walls at a uniform temperature of 1000 K was considered. Figure 2 shows the results of the calculations for different sensor locations inside the cavity, for three values of the sensor-holder size.

When the sensor is close to the cavity base ($x/d_c = 0$), the internal reflections of the rays within the cavity do not reach the sensor. Hence, the effective emissivity (ε_{eff}) will be close to the cavity-wall emissivity (ε_c), or somewhat higher. When the sensor is moved away from the cavity base, the effective emissivity increases rapidly, up to a distance of about $x/d_c = 0.5$, due to the contribution of reflected rays within the cavity reaching the sensor surface. Reduction of the holder size for a specified wall emissivity also results in a steeper increase in the effective emissivity near the cavity base.

For sensor locations $x/d_c > 0.5$, the effective emissivity increases gradually with distance and reaches a limiting value at a distance of about one cavity diameter from the base. The increase beyond $x/d_c > 1$ is not significant. In the range $x/d_c = 1$–4, the effective emissivity is nearly uniform and drops slightly near the exit region due to the annular opening. These results demonstrate that the dominant effect determining the effective emissivity of an isothermal cavity is the wall emissivity close to the cavity base and close to the open end near the cavity exit. In between, a region of nearly uniform effective emissivity exists for isothermal-cavity conditions. However, the value of the calculated emissivity in the uniform region depends on the cavity-wall emissivity and the sensor-holder diameter.

The observed trend in effective emissivity variation with distance is similar for all wall emissivity values $\varepsilon_c = 0.7$, 0.8, and 0.9. With a decrease in holder size, the effective emissivity value in the uniform zone increases rapidly. For $d_h/d_c = 0.25$, the effective emissivity value is about 0.988 for $\varepsilon_c = 0.7$, and 0.998 for $\varepsilon_c = 0.9$. The corresponding values for $d_h/d_c = 0.25$ are 0.954 and 0.988 for $\varepsilon_c = 0.7$ and 0.9, respectively. Typical variation with holder size at a fixed location of sensor corresponding $x/d_c = 1.0$ is shown in Fig. 3. These
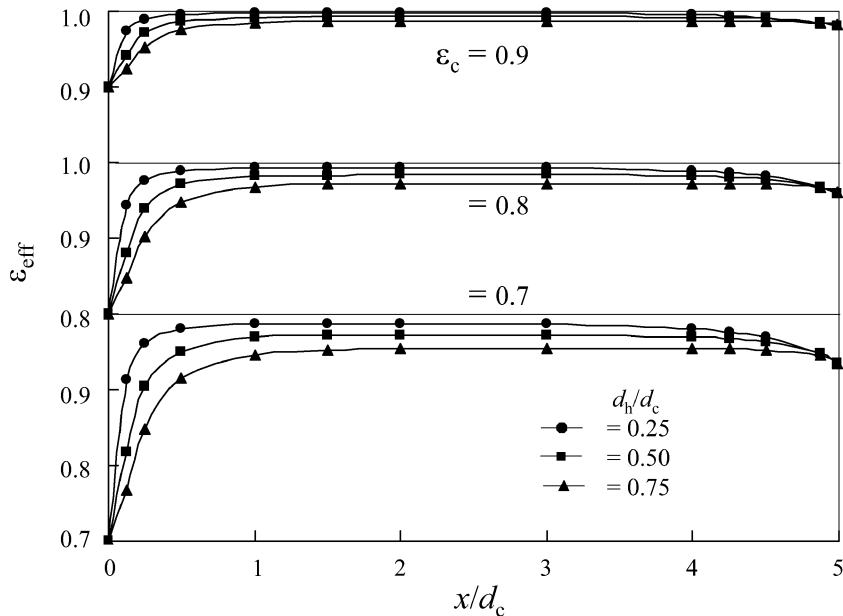
Fig. 2   Effective emissivity inside a diffuse cylindrical isothermal cavity ($\varepsilon_h = 0.5$ and $\varepsilon_s = 0.95$).
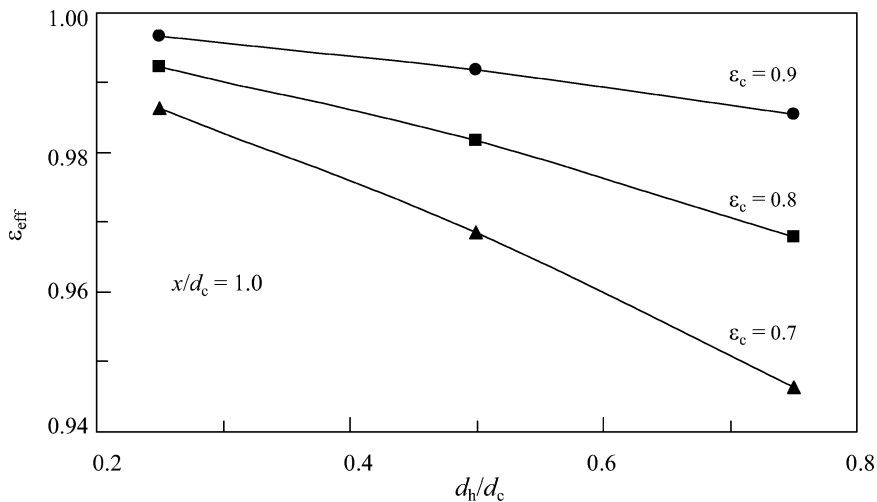

Fig. 3   Holder size effect on effective emissivity for isothermal cavity at $x/d_c = 1$ ($\varepsilon_h = 0.5$ and $\varepsilon_s = 0.95$).

calculations demonstrate the need to keep the holder size as small as possible to achieve a high value of effective emissivity at the sensor location.

Because of the absence of data on cavity-wall diffusity, we performed a numerical study for different values of D in the range 0–1. Figure 4 shows the influence of diffusity on the effective emissivity for values of $d_h/d_c = 0.25$, 0.50, and 0.75, and $\varepsilon_c = 0.7$, 0.8, and 0.9 corresponding to isothermal cavity-wall temperature distribution. The results demonstrate the weak dependences of effective emissivity on wall diffusity. For $\varepsilon_c = 0.7$ and $d_h/d_c = 0.25$, the effective emissivity increases from 0.978 to 0.982 for diffusity values of 0.5 and 1.0, respectively. The change is much lower with increasing holder diameter and higher cavity-wall surface emissivity. These calculations confirm the well-established thesis[13] that for cavities with small values of aperture-to-inner surface ratio, the angular distribution of reflected radiation has little influence on the calculated effective emissivity value.

Nonisothermal Cavity

The foregoing calculations refer to a cavity with uniform temperature distribution on the internal surface. However, practical blackbodies deviate from isothermal conditions due to nonuniform heat-ing and cooling conditions and often exhibit a temperature gradient along the cavity length. To study the influence of nonuniform temperature distribution on the effective emissivity, calculations were performed under the assumption of a linear temperature decrease along the cavity length.

Figure 5 shows the temperature distribution used for nonisothermal calculations. Over the cavitybase (A–B), the distribution was uniform at 1000 K. The variation from the cavitybase (B) to the exit (C) was linear with the temperature at the exit location (C), specified at 980, 960 and 940 K. The distribution was uniform at 300 K over the other segments of the boundary (C–F).

Figure 6 shows the results of the calculated effective emissivity for three values of the cavity surface emissivity and different locations inside the cavity, for both isothermal and non-isothermal conditions. The results presented correspond to the case when the holder diameter is one-half of the cavity diameter ($d_h/d_c = 0.5$), with the holder and sensor surface emissivity values of 0.5 and 0.95, respectively. The cavity base temperature (1000 K) was used as reference to calculate the effective emissivity.

In the region close to the cavity base up to $x/d_c \approx 0.5$, the temperature gradient has little effect on the calculated emissivity and is dependent only on the cavity-wall emissivity ε_c. As can be expected,
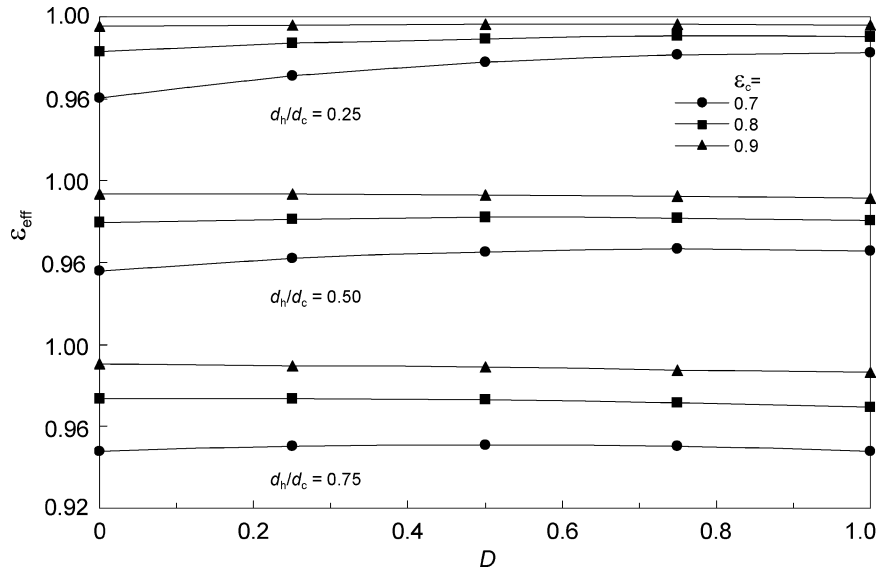
Fig. 4   Wall diffusity influence on effective emissivity for isothermal cavity at x/d_c = 0.5 (T_c = 1000 K).
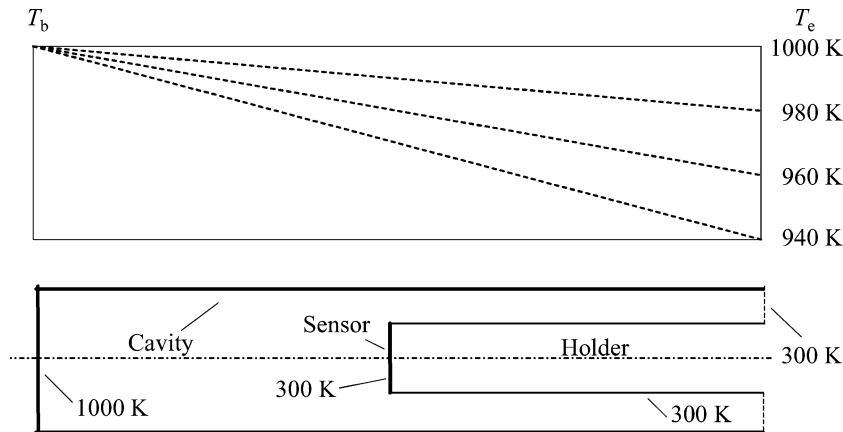

Fig. 5   Temperature distribution for nonisothermal conditions.

an increase in ε_c results in a higher effective emissivity for a given location. The effective emissivity peaks in the region $x/d_c \approx 0.5$ and then decreases away from the base when the temperature gradient effects are included. As mentioned before, in the range $x/d_c = 1$–4, the effective emissivity is nearly uniform only for the isothermal case. The drop from the isothermal cavity values is a strong function of the temperature gradient and the distance away from the base. At location $x/d_c = 2.0$, even with a low-temperature gradient corresponding to 980 K at the cavity exit and a wall emissivity $\varepsilon_c = 0.9$, the effective emissivity drops to 0.972 from the isothermal value of 0.993.

Figure 7 shows the relative change in the effective emissivity with respect to the isothermal value for location $x/d_c = 0.5$, 1.0, and 2.0. The relative change from an isothermal value was weakly dependent on the wall emissivity in the range 0.7–0.9 corresponding to graphite material.

These results suggest that, for a nonisothermal cavity, whereas cavity wall emissivity dominates near the base, the nonuniform temperature distribution significantly affects the effective emissivity away from the base. Because it is more likely that practical blackbodies have or develop temperature gradients, the results suggest that the region $x/d_c \approx 0.5$ represents a suitable location where the effective emissivity is least influenced by temperature gradient effects. The results presented in Fig. 7 correspond to the case of $d_h/d_c = 0.5$. Similar behavior was also noted for $d_h/d_c = 0.25$ and 0.75.

Holder Emissivity Effects

The holder surface emissivity ε_h influences the irradiance at the sensor surface by affecting the magnitude of internal reflections reaching the sensor. It is desirable to have a highly reflective surface (low emissivity) for the holder to ensure a high value of the effective emissivity. The isothermal and nonisothermal results discussed earlier correspond to a holder emissivity value $\varepsilon_h = 0.5$. The effect of variation of the holder emissivity on the effective emissivity at location $x/d_c = 1$ is shown in Fig. 8 for both isothermal and nonisothermal cavity conditions. The corresponding cavity emissivity was 0.8, and the holder to cavity diameter ratio was 0.5. With increasing holder emissivity from 0.1 to 0.7, the effective emissivity decreases almost linearly for the isothermal and nonisothermal cavity conditions considered. The decrease from the isothermal value is about 0.005 and is nearly the same for all of the cases considered.

Implications for Testing

The parametric studies highlight the important factors that need consideration during calibration at high heat-flux levels by placement of the sensor inside a heated blackbody cavity. For the cylindrical cavity shape commonly used for high temperatures, it is desirable to place the sensor at a location where the influence of temperature gradient and the emissivity of the cavity-wall surface are minimal on the effective emissivity.

Close to the cavity base, the influence of the temperature gradient along the cavity length on the calculated emissivity is small.
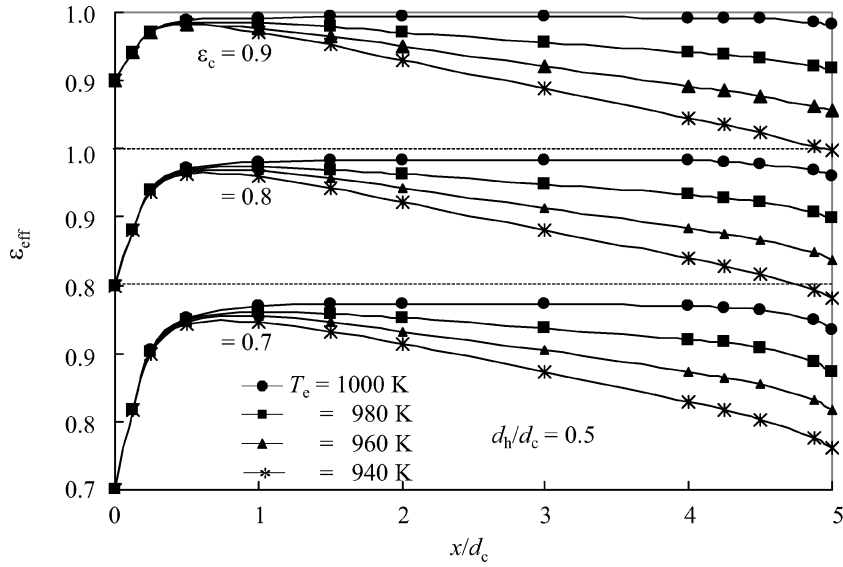
Fig. 6 Effective emissivity inside a nonisothermal cylindrical cavity ($\varepsilon_h = 0.5$ and $\varepsilon_s = 0.95$).
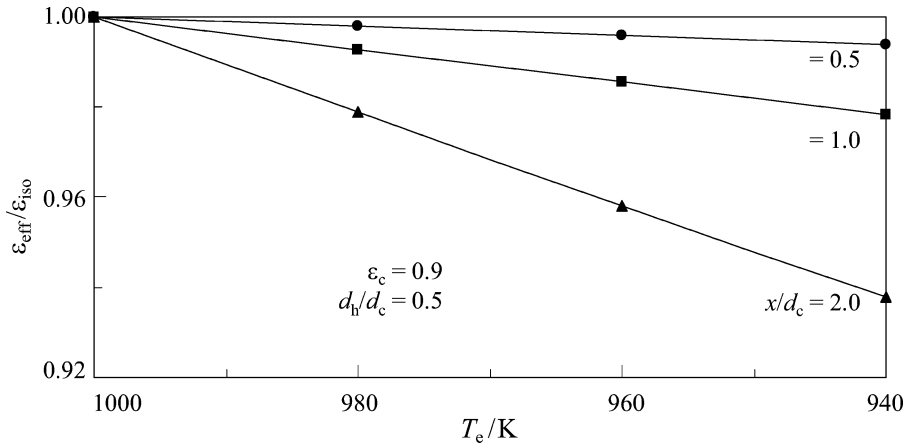

Fig. 7 Change in effective emissivity from isothermal value for linear wall temperature variation ($\varepsilon_h = 0.5$ and $\varepsilon_s = 0.95$).
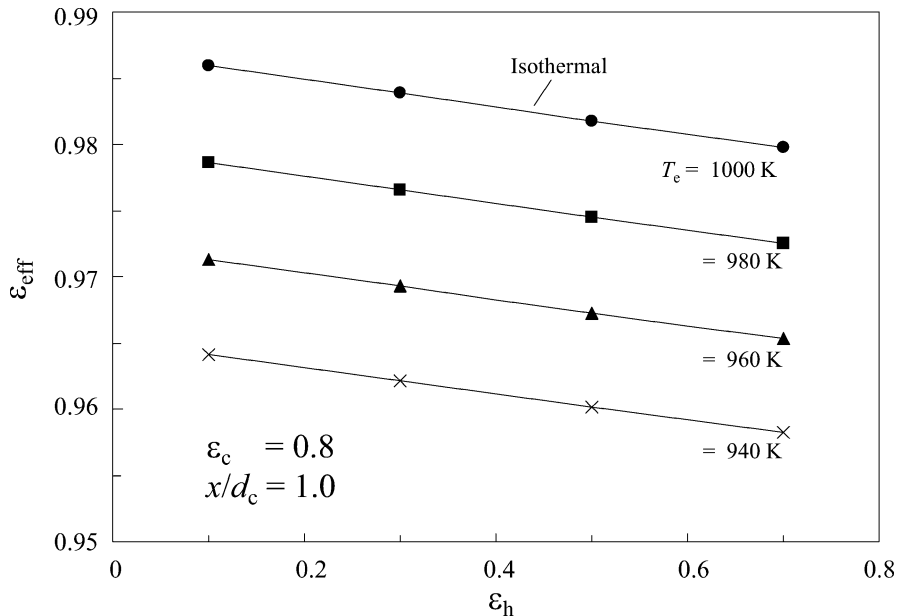

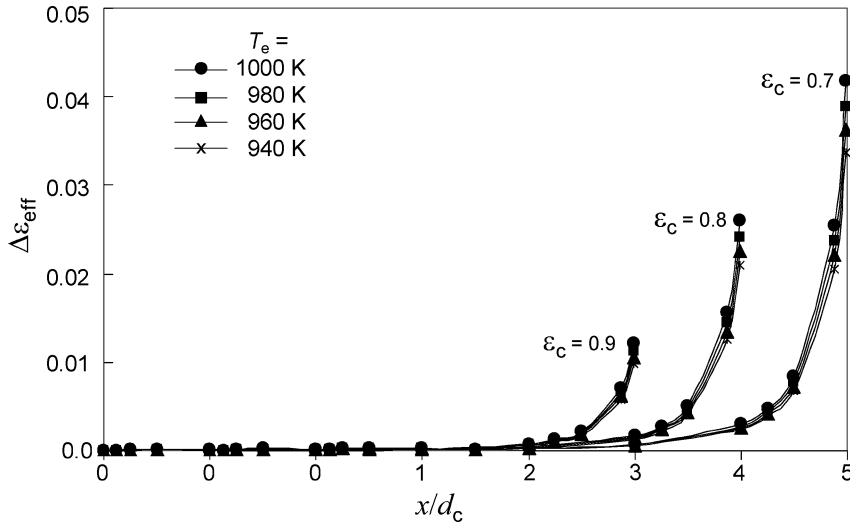**Fig. 8** Holder emissivity influence on effective emissivity at $x/d_c = 1$ ($\varepsilon_s = 0.95$).

Fig. 9   Effective emissivity increase with a reflecting shield (ρ_{sh} = 0.9) at the blackbody exit.

However, the effective emissivity in this region is significantly lower than unity and highly sensitive to the location because of the rapid rise in magnitude when it is moved away from the base. A previous study[14] reports experiments on a sensor with a 12.5-mm holder in a 25-mm-diam cavity at a distance of 3 mm from the cavity base. A blackbody radiation environment, with an effective emissivity of unity, was assumed at this location. The present calculations show that such an assumption can result in an overestimate of the irradiance at the sensor location. The emissivity of graphite material used for the cavity wall can show a large spectral variation. Despite this variation, the effective emissivity at a distance of about one radius from the base does not change significantly. The effective emissivity at this location, although significantly higher, will still be lower than unity and needs to be determined for the specific experimental conditions.

Calculations with different holder sizes show that the smaller the holder size, the higher the effective emissivity will be at a given location. However, there may be other practical limitations. During testing, the insertion and removal of the cold sensor holder into the heated cavity is for a short duration. If the holder size is large, the holder can introduce severe thermal loading on the blackbody heating system and likely will disturb the equilibrium conditions. The thermal loading effect is facility dependent and difficult to asses theoretically. Given this, it is desirable to minimize cavity temperature variations during test duration by gradual insertion of the holder and by the use of a smaller holder diameter compared to the cavity size. A holder to cavity diameter ratio of 0.25 is a suitable choice.

The analysis assumes that the reference value for calculation of the effective emissivity is the cavity back surface measured temperature, which is usually the parameter used to control the blackbody operation. However, the temperature at any other location can be used as a reference to define the effective emissivity and the appropriate temperature distribution used in the calculations. In an actual calibration, the insertion of the sensor close to the cavity disturbs the equilibrium conditions by cooling the wall. The control system, although stabilizing the temperature to the set value at the control location, drives the temperature to higher values along the cavity length. The present analysis shows that such effects should have minimal influence on the effective emissivity when the sensor location is at a distance of about one cavity radius from the end. In situations when the influence is not small, the analysis will be helpful in the determination of the uncertainty in the effective emissivity value based on expected temperature change.

Enhancing Effective Emissivity

This section examines the possibility of an increase of the effective emissivity by modifications to the blackbody. Two well-known approaches to enhance the emissivity are the use of a grooved cavity surface for the blackbody or a reflecting shield. These modifications increase the number of internal ray reflections within the cavity, which leads to increased effective emissivity. Of the two approaches, a reflecting shield is simple and does not involve extensive modifications to the blackbody.

It is possible to determine the effect of a reflecting shield by the use of the shield reflectance value for the annular exit region between the holder and the cavity, instead of the perfect blackbody assumption. Although we will not discuss the details of practical implementation for such an annular shield, we will assume that the shield temperature is 300 K. Figure 9 shows the increase in the effective emissivity at different locations inside the cavity, due to the reflecting shield at the exit, compared to earlier calculations with a perfect blackbody assumption.

The results shown correspond to a holder to cavity diameter ratio of 0.5 for values of $\varepsilon_c = 0.7$, 0.8, and 0.9. The values of other geometric parameters remain the same as before. The increase in the effective emissivity is highest at the shield plane and decreases rapidly away from the shield. Beyond a distance of about one cavity diameter, the increase in effective emissivity is negligible. This trend holds for all three values $\varepsilon_c = 0.7$, 0.8, and 0.9 and for both uniform and linearly varying cavity-wall temperature distributions. The increase in effective emissivity becomes larger with increasing ε_c. These calculations show that the reflecting shield is most beneficial when the measurement location is in the shield plane. An example of this particular case is in the measurement of radiance temperature in rapid thermal processing.[15] However, the use of a reflecting shield in the exit plane does not help when the measurement location is inside the cavity.

The end surface of the sensor holder housing the heat-flux sensing element normally has high absorptance black paint to absorb the incident radiation. In the preceding calculations, a value of $\varepsilon_s = 0.95$ was assumed for the end surface. However, it is advantageous to limit the application of high absorptance paint to the sensing area only and to have the surrounding area remain highly reflective. Figure 10 shows the comparison between the two cases under the assumption of a reflectance value of 0.9 for the surrounding area for different sensor locations inside the cavity and for $\varepsilon_c = 0.8$. When the sensor is close to the cavity bottom, the increase in effective emissivity is large, with a reflective surrounding region around the sensing area. However, the effectiveness decreases when the sensor is away from the cavity bottom. The effective emissivity increase remains nearly constant for sensor locations $x/d_c > 1$. Figure 11 shows the increase in the effective emissivity for different values of ε_c. The curves for the isothermal cavity and for different cavity temperature distributions merge. Thus, the effective emissivity increase is practically independent of ε_c for all locations and is
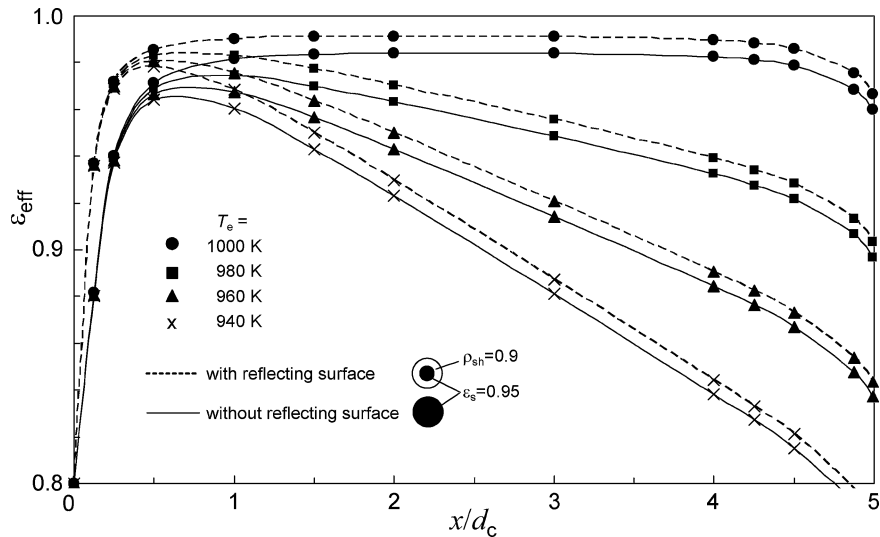
Fig. 10 Effective emissivity with and without reflecting surface in the sensor plane ($\varepsilon_c = 0.8$).
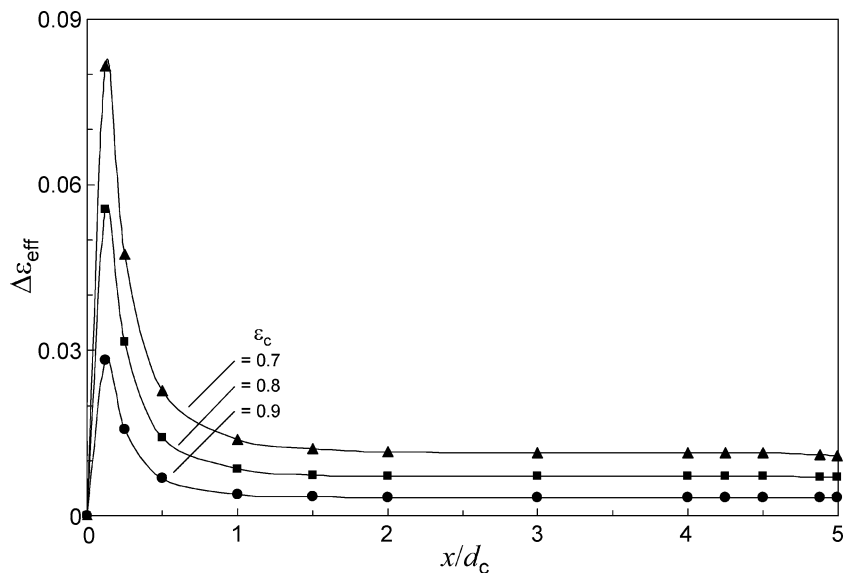

Fig. 11 Effective emissivity increase with reflecting surface ($\rho_{sh} = 0.9$) in the sensor plane.

nearly same for both the isothermal and linearly varying temperature distributions.

Conclusions

A Monte Carlo approach to determine the effective emissivity inside a heated cylindrical cavity in the presence of a cooled sensor holder is presented. The computations, carried out in support of a high heat-flux sensor calibration, demonstrated the effect of cavity wall emissivity, temperature gradient, and sensor-holder size and absorptance on the calculated effective emissivity. Movement of the sensor location away from the cavity base resulted in a rapid increase in the effective emissivity. At a distance of about one cavity radius, the effective emissivity reaches a peak, and its variation with temperature nonuniformity or positioning accuracy is small in this region. Therefore, the results suggest that the optimum location for the sensor calibration is about one cavity radius from the cylindrical cavity base. For a given location inside the cavity, the effective emissivity increases with decreasing sensor-holder size because of an increased number of reflections reaching the sensor surface.

A sensor-holder to cavity diameter ratio of 0.25 appears to be a good choice for tests to maximize the effective emissivity and reduce thermal loading of the blackbody heating system. An increase of the holder emissivity from 0.1 to 0.7 decreased the effective emissivity by only about 0.5% for both isothermal and nonisothermal conditions. Provision of a reflecting surface around the high absorptance region of the sensor surface increases the effective emissivity value. By proper choice of a holder size and a highly reflecting surface, it is possible to minimize the correction for the effective emissivity. At a distance of about one cavity radius from the cavity bottom, the calculated effective emissivity is as high as 0.99, which is close to the theoretical value of unity. Of the various effects present, the cavity-wall temperature gradients play the most significant role in determining the effective emissivity. Calculations specific to the experimental conditions are necessary to determine the correct heat flux at the sensor location inside the heated blackbody cavity.

References

[1]Murthy, A. V., Tsai, B. K., and Saunders, R. D., "High Heat Flux Sensors Calibration using Blackbody Radiation," *Metrologia*, Vol. 35, No. 4, 1998, pp. 501–504.

[2]Murthy, A.V., Tsai, B. K., and Saunders, R. D., "NIST Radiative Heat Flux Sensor Calibration Facilities and Techniques," *Journal of Research of the National Institute of Standards and Technology*, Vol. 105, No. 2, 2000, pp. 293–305.

[3]Bedford, R. E., "Calculation of Effective Emissivities of Cavity Sources of Thermal Radiation," *Theory and Practice of Radiation Thermometry*, edited by D. P. DeWitt and G. D. Nutter, Wiley, New York, 1988, pp. 653–772.

[4]Ono, A., "Calculation of the Directional Emissivities of Cavities by the Monte Carlo Method," *Journal of the Optical Society of America*, Vol. 70, No. 5, 1980, pp. 547–554.

[5]Sapritsky, V. I., and Prokhorov, A. V., "Calculation of the Effective Emissivities of Specular-Diffuse Cavities by the Monte Carlo Method," *Metrologia*, Vol. 29, No. 1, 1992, pp. 9–14.

[6]Chu, Z., Dai, J., and Bedford, R. E., "Monte Carlo Solution for the Directional Effective Emissivity of a Cylindro-inner Cone," *Proceedings of the American Institute of Physics*, edited by J. F. Schooley, Vol. 6, No. 1, American Inst. of Physics, New York, 1992, pp. 907–912.

[7]Prokhorov, A. V., and Martin, J. E., "Monte Carlo Simulation of the Radiative Heat Transfer from a Blackbody to a Cryogenic Radiometer," *Proceedings of SPIE — The International Society for Optical Engineering*, Society of Photo-Optical Instrumentation Engineers, Bellingham, WA, Vol. 2815, 1996, pp. 160–168.

[8]Ballico, M. J., "Modeling of the Effective Emissivity of a Graphite Tube Blackbody," *Metrologia*, Vol. 32, No. 4, 1995/1996, pp. 259–265.

[9]Sapritsky, V. I., and Prokhorov, A. V., "Spectral Effective Emissivities of Non-isothermal Cavities Calculated by the Monte Carlo Method," *Applied Optics*, Vol. 34, No. 25, 1995, pp. 5645–5652.

[10]*STEEP3, Version 1.3. User's Guide*, Virial, Inc., New York, 2000.

[11]Prokhorov, A. V., "Monte Carlo Method in Optical Radiometry," *Metrologia*, Vol. 35, No. 4, 1998, pp. 465-471.

[12]Prokhorov, A. V., Hanssen, L, M., and Mekhontsev, S. N., "Reciprocity Principle and Choice of the Reflectance Model for Physically Correct Modeling of Effective Emissivity," *Temperature: Its Measurement and Control in Science and Industry*, edited by D. C. Ripple, Vol. 7, American Institute of Physics, New York, 2003, pp. 729–734.

[13]Quinn, T. J. *Temperature—Monographs in Physical Measurement Series*, 2nd ed., Academic Press, New York, 1990, p. 349.

[14]Brookley, C. E., and Llewellyn, W. E., "Determination of Blackbody Radiance at Temperatures above 2300°C," *Temperature: Its Measurement and Control in Science and Industry*, edited by J. F. Schooley, Vol. 6, American Inst. of Physics, New York, 1992, pp. 1195–1199.

[15]Zhou, Y. H., Shen, Y. J., Zhang, Z. M., Tsai, B. K., and DeWitt, D. P., "A Monte Carlo Model for Predicting the Effective Emissivity of the Silicon Wafer in Rapid Thermal Processing Furnaces," *International Journal of Heat and Mass Transfer*, Vol. 45, No. 9, April 2002, pp. 1945–1949.